



## Effect of indium doping on structural, magnetic and transport properties of ordered $\text{Sr}_2\text{FeMoO}_6$ double perovskite

Y. Markandeya<sup>a</sup>, D. Saritha<sup>a</sup>, M. Vithal<sup>b</sup>, A.K. Singh<sup>c</sup>, G. Bhikshamaiah<sup>a,\*</sup>

<sup>a</sup> Department of Physics, Osmania University, Hyderabad 500007, India

<sup>b</sup> Department of Chemistry, Osmania University, Hyderabad 500007, India

<sup>c</sup> Defence Metallurgical Research Laboratory (DMRL), Hyderabad 500058, India

### ARTICLE INFO

#### Article history:

Received 2 January 2011

Received in revised form 6 February 2011

Accepted 7 February 2011

Available online 5 March 2011

#### Keywords:

Oxide materials

Sol–gel process

X-ray diffraction

Crystal structure

Magnetic measurements

Magnetoresistance

### ABSTRACT

A series of  $\text{Sr}_2\text{Fe}_{1-x}\text{In}_x\text{MoO}_6$  ( $x=0, 0.1, 0.3$  and  $0.4$  wt.%) (SFIMO) double perovskite oxide powders were prepared by sol–gel method. The materials were subjected to X-ray diffraction and found to crystallize in tetragonal structure with space group  $I4/mmm$ . Lattice parameters and unit cell volume were calculated using X-ray diffraction data. It was found that the tetragonal distortion ( $c/a\sqrt{2}$ ) increases while the deviation of the tolerance factor from unity increases with increase of indium composition in SFIMO samples. Magnetization studies were carried out using vibrating sample magnetometer (VSM). It has been found that the saturation magnetization ( $M_s$ ) and remanent magnetization ( $M_r$ ) decreases while coercivity ( $H_c$ ) increases with increase of indium composition in SFIMO samples. Electrical resistivity and magnetoresistance studies in the magnetic field range from  $-40$  kOe to  $40$  kOe were carried out keeping the temperature constant at  $5, 150$  and  $300$  K using standard four-probe method. Resistivity studies were also performed in the temperature range from  $5$  to  $300$  K keeping magnetic field constant at  $0, 10, 20$  and  $40$  kOe. The resistivity studies showed that the magnitude of magneto resistance (MR%) decreases with increase of temperature from  $5$  to  $300$  K while the value of MR (%) is found to increase with increase of magnetic field. The MR (%) was found to decrease with increase of indium concentration in SFIMO compounds. The degree of ordering,  $M_s$  and MR (%) agreed well with each other.

© 2011 Elsevier B.V. All rights reserved.

### 1. Introduction

A survey of literature shows that the double perovskite of type  $A_2\text{BB}'\text{O}_6$  ( $A=\text{Sr}, \text{Ca}, \text{Ba}$ ;  $B=\text{Fe}, \text{Cr}, \text{Ga}, \text{Mg}, \text{Mn}, \text{etc.}$ ; and  $B'=\text{Mo}, \text{Re}, \text{W}, \text{etc.}$ ) were extensively studied for the past several years due to the substantial low field magnetoresistance (MR) that was initially reported at room temperature for  $\text{Sr}_2\text{FeMoO}_6$  (SFMO) [1]. The  $\text{Sr}_2\text{FeMoO}_6$  compound crystallizes in tetragonal lattice with space group  $I4/mmm$  [2]. The structure of  $\text{Sr}_2\text{FeMoO}_6$  can be viewed as a regular arrangement of corner-sharing  $\text{FeO}_6$  and  $\text{MoO}_6$  octahedra, alternating along the three directions of the crystal, with the Sr cations occupying the voids in between the octahedra [1]. The ferromagnetic structure of SFMO can be described as an ordered array of parallel  $\text{Fe}^{3+}$  ( $S=5/2$ ) magnetic moments, antiferromagnetically coupled with  $\text{Mo}^{5+}$  ( $S=1/2$ ) spins. According to this model the  $M_s$  of SFMO should be  $4 \mu_B$ . However, most of the experiments show a reduced  $M_s$  due to the anti-site disorder at B and B' sites [3–5]. In the presence of anti-site defects (ASDs), some Fe ions in

Mo sites interact with its neighboring Fe ions exhibiting antiferromagnetism (AFM), leading to reduction in  $M_s$  [6]. A remarkable negative MR (%) at low fields has been observed for  $\text{Sr}_2\text{FeMoO}_6$  even at room temperature. The origin of low-field MR (LFMR) in polycrystalline samples in the double perovskite materials has been attributed to the spin-dependent scattering of electrons at grain boundary. It is also reported that the LFMR of  $\text{Sr}_2\text{FeMoO}_6$  increase with the decrease of ASDs [7]. Therefore, ASDs among the B and B' sites have large influence on the magnetic and transport properties of  $\text{Sr}_2\text{FeMoO}_6$ . Several investigations on cationic doping at both Sr and Mo sites were carried out in order to explore and tailor LFMR in  $\text{Sr}_2\text{FeMoO}_6$  [8–10]. But the magnetic structure, especially the ASDs, can be modified notably by doping at Fe site [6]. Consequently, the substitution at Fe site will be more helpful in understanding the correlation between magnetic structure and magnetotransport properties of SFMO. Therefore, several investigations were carried out in order to understand the correlation between the degree of Fe/Mo ordering, magnetic structure and MR (%) of  $\text{Sr}_2\text{FeMoO}_6$  by doping with elements such as Ni, Cr, V, Cu, Mn, Ga, Co, Mg and Al at Fe site [6,11–22]. However, doping of indium at Fe site in  $\text{Sr}_2\text{FeMoO}_6$  is not investigated so far. In view of this, the authors have taken up the present work with an objective to study the effect of indium doping at Fe site on the structural, magnetic and

\* Corresponding author at: Department of Physics, Osmania University, H.NO.3-18-218, Pragathi Nagar, Ramanthapur, Hyderabad, India. Tel.: +91 9949565350.

E-mail address: [gbhyd08@gmail.com](mailto:gbhyd08@gmail.com) (G. Bhikshamaiah).

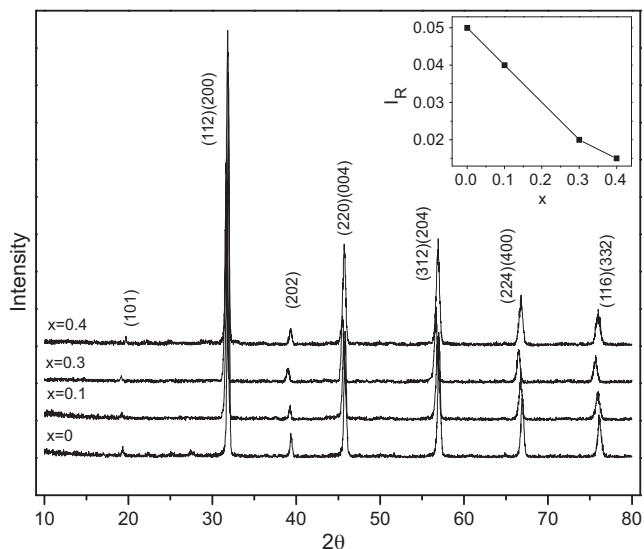


**Fig. 1.** X-ray diffraction patterns of  $\text{Sr}_2\text{Fe}_{1-x}\text{In}_x\text{MoO}_6$  ( $x=0, 0.1, 0.3$  and  $0.4$  wt.%) samples recorded at room temperature are shown along with  $(hkl)$  values. Inset figure shows the variation of observed relative intensity ratio ( $I_R = I_{(101)} / [I_{(112)} + I_{(200)}]$ ) with indium composition.

magnetotransport properties of ordered  $\text{Sr}_2\text{FeMoO}_6$  double perovskite.

## 2. Experimental details

Various compositions of  $\text{Sr}_2\text{Fe}_{1-x}\text{In}_x\text{MoO}_6$  ( $x=0, 0.1, 0.3$  and  $0.4$  wt.%) (SFIMO) have been synthesized by sol-gel method [23–25]. Stoichiometric amount of AR grade  $\text{Sr}(\text{NO}_3)_2$ ,  $\text{Fe}(\text{NO}_3)_3 \cdot 9\text{H}_2\text{O}$ ,  $\text{In}_2\text{O}_3$  and  $\text{H}_2\text{MoO}_4$  are taken in beaker and about 200 ml distilled water is added. Citric acid is added to this mixture such that the mole ratio of citric acid to metal ions is 2:1. Then dilute ammonia solution is added to adjust the pH of the solution to 7. Then the beaker containing the solution is heated on hot-plate of magnetic stirrer at  $80^\circ\text{C}$  for about a day. Ethylene glycol is added to this solution such that metal ion to ethylene glycol ratio is 1:1.2 and heated until a dark brown gel is formed. This gel is then heated for about 5 min at  $250^\circ\text{C}$  using Bunsen burner to get dried powders. The dried brown powder was then taken into a crucible and heated at  $500^\circ\text{C}$  for 6 h in a Furnace. The powder was heated at  $700^\circ\text{C}/6\text{h}$ ,  $900^\circ\text{C}/6\text{h}$  and  $1100^\circ\text{C}/6\text{h}$  with intermittent grinding. These powders are then pressed into pellets of 1 cm diameter and about 2 mm thickness using a die and a hydraulic press by applying a pressure of 1 t. These pellets were then sintered at  $1200^\circ\text{C}$  for 6 h. Subsequently, these pellets were heated at  $1000^\circ\text{C}$  in a stream mixture of 10%  $\text{H}_2/\text{Ar}$  gas for about 3 h for loss of oxygen or reducing the  $\text{Mo}^{6+}$  to  $\text{Mo}^{5+}$  and/or  $\text{Fe}^{3+}$  to  $\text{Fe}^{2+}$ . These materials are subjected to X-ray diffraction studies using Philips PW 1830 generator diffractometer with  $\text{Cu K}\alpha$  radiation ( $40\text{ kV} \times 25\text{ mA}$ ) and a graphite monochromator in order to confirm the structure. The magnetization measurements of  $\text{Sr}_2\text{Fe}_{1-x}\text{In}_x\text{MoO}_6$  ( $x=0, 0.1, 0.3$  and  $0.4$  wt.%) samples were measured as a function of magnetic field from  $-15\text{ kOe}$  to  $15\text{ kOe}$  at room temperature using Digital Measurement Systems' Model 880 USA make of Vibrational Sample Magnetometer. Electrical resistivity measurements were carried out at constant magnetic field of 0, 10, 20 and 40 kOe in the temperature range 5–300 K employing the standard four-probe method with the use of a superconducting magnet system of OXFORD. The resistivity measurements were also carried out keeping temperature constant at 5, 150 and 300 K while varying magnetic field from  $-40\text{ kOe}$  to 40 kOe. The relevant MR (%) has been evaluated using this resistivity data as a function of temperature as well as magnetic field.

## 3. Result and discussion

### 3.1. Crystal structures

The X-ray diffraction (XRD) patterns of  $\text{Sr}_2\text{Fe}_{1-x}\text{In}_x\text{MoO}_6$  ( $x=0, 0.1, 0.3$  and  $0.4$  wt.%) (SFIMO) are shown in Fig. 1. All the XRD profiles of  $\text{Sr}_2\text{Fe}_{1-x}\text{In}_x\text{MoO}_6$  were indexed and found to crystallize in double perovskite structure with tetragonal space group  $I4/mmm$ . The  $(hkl)$  values of indexed reflections are also shown in Fig. 1. All the SFIMO compounds exhibited a superstructure peak (101) which arises from the ordered arrangement of Fe and Mo ions in

the double perovskite. When Fe ions occupy the Mo site and vice versa, the ordering of Fe and Mo ions will be disturbed leading to anti-site defects (ASDs) which are sensitive to synthesis conditions [6]. It has been found that the intensity of super structure reflection (101) decreases with increase of indium composition. Therefore, the relative intensity ratio of the superstructure peak  $I_R = I_{(101)} / [I_{(112)} + I_{(200)}]$  was calculated and variation of  $I_R$  with indium composition is shown in the inset of Fig. 1. It shows that the  $I_R$  decreases indicating decrease of degree of Fe/Mo ordering or increase of ASDs with increase of indium composition in SFIMO samples. Similar results were reported when Ni is doped at Fe site in SFMO [6]. The lattice parameters  $a$  and  $c$  of SFIMO compounds were calculated using (101), (112), (202), (220), (312), (224) and (116) X-ray diffraction profiles and are given in Table 1. The lattice parameters  $a$  and  $c$  are found to be in the range  $5.56\text{--}5.62\text{ \AA}$  and  $7.90\text{--}7.97\text{ \AA}$  respectively. The volume of unit cell of SFIMO compounds was also calculated using the relation  $V = 2a^2c$  and included in Table 1. The volume of unit cell of SFIMO is found to vary between  $492.34\text{ \AA}^3$  and  $499.83\text{ \AA}^3$ . It is found that there is no systematic variation of lattice parameters  $a$ ,  $c$  and unit cell volume with increase of indium composition in SFIMO compounds. Since the ionic radius of  $\text{In}^{3+}$  ( $0.79\text{ \AA}$ ) ion is larger than  $\text{Fe}^{3+}$  ( $0.645\text{ \AA}$ )/ $\text{Fe}^{2+}$  ( $0.78\text{ \AA}$ ) ions, the random variation in lattice parameter or unit cell volume might be attributed to cation or oxygen vacancies as observed in many perovskites [26–28] or valence disproportion. Tetragonal lattice distortion ( $c/a\sqrt{2}$ ) of SFIMO compounds was calculated using lattice parameters  $a$  and  $c$  and shown in Table 1. It is found that the tetragonal distortion is generally found to increase with indium composition indicating reduction in the symmetry of the lattice on substitution of  $\text{In}^{3+}$  for  $\text{Fe}^{3+}/\text{Fe}^{2+}$ .

The tolerance factor ( $t$ ) is a semi quantitative estimate of how close an  $\text{ABO}_3$  perovskite is to the cubic structure; moreover, the tolerance factor indicates stability of the perovskite structure, that is, the higher is the deviation of tolerance factor ( $t$ ) from unity, lesser is the stability of perovskite structure. The tolerance factor for  $\text{ABO}_3$  perovskite structure is given by

$$t = \frac{r_A + r_O}{\sqrt{2}(r_B + r_O)} \quad (1)$$

where  $r_A$ ,  $r_B$  and  $r_O$  are the ionic radii of A, B and Oxygen atoms respectively and  $t = 1$  corresponds to an ideal cubic perovskite structure. The concept of tolerance factor ( $t$ ) has been extended to  $\text{A}_2\text{B}_{(1-x)}\text{B}'_x\text{B}'_0\text{O}_6$  double perovskites by Lu et al. [19] and is given by

$$t = \frac{r_A + r_O}{\sqrt{2}((r_B(1-x)/2) + (r_{B'}x/2) + (r_{B'}/2) + r_O)} \quad (2)$$

where  $r_A$ ,  $r_B$ ,  $r_{B'}$ ,  $r_{B'}$  and  $r_O$  are ionic radii of the respective ions. They have evaluated tolerance factor of  $\text{Sr}_2\text{Fe}_{1-x}\text{Ga}_x\text{MoO}_6$  using Eq. (2) and described symmetry of lattice. In the present study, the tolerance factor ( $t$ ) for SFIMO compounds was calculated employing Eq. (2) and the values are included in Table 1. It may be noted that the tolerance factor ( $t$ ) decreases with increase of indium composition indicating distortion of lattice from double perovskite structure. Thus addition of indium at Fe site in  $\text{Sr}_2\text{FeMoO}_6$  reduces the symmetry of lattice.

### 3.2. Magnetization measurements

Magnetic field dependence of magnetization of  $\text{Sr}_2\text{Fe}_{1-x}\text{In}_x\text{MoO}_6$  compounds ( $x=0, 0.1, 0.3$  and  $0.4$  wt.%) taken at 300 K is shown in Fig. 2. The values of  $M_s$ ,  $M_r$  and  $H_c$  for all the compounds were obtained from Fig. 2 and given in Table 1. The variation of  $M_s$  with indium composition is shown in left side inset in Fig. 2. It can be seen from the inset of Fig. 2 that the  $M_s$  decreases with increase of indium content in SFIMO samples. The value of

**Table 1**  
Crystallographic, magnetic parameters and MR (%) values of  $\text{Sr}_2\text{Fe}_{1-x}\text{In}_x\text{MoO}_6$  ( $x=0, 0.1, 0.3$  and  $0.4$  wt.%) double perovskites.

Composition (x) wt.%	0	0.1	0.3	0.4
Lattice parameter [ $a$ (Å)]	5.57	5.62	5.56	5.60
Lattice parameter [ $c$ (Å)]	7.90	7.93	7.97	7.92
Unit cell volume [ $V$ (Å <sup>3</sup> )]	493.28	499.83	492.34	497.24
Tetragonal lattice distortion [ $(c/a\sqrt{2})$ ]	2.3648	2.3654	2.3889	2.3663
Tolerance factor ( $t$ )	0.9906	0.9870	0.9801	0.9766
Saturation magnetization [ $M_s$ (e.m.u./g)]/ $T=300$ K	18.07	11.67	10.00	4.13
Coercivity [ $H_c$ (Oe)]/ $T=300$ K	39	50	65	68
Remanent magnetization [ $M_r$ (e.m.u./g)]/ $T=300$ K	0.38	0.12	0.04	0.02
MR (%)/ $T=5$ K, $H=10$ kOe	-12.01	-6.18	-1.08	-2.78
MR (%)/ $T=5$ K, $H=20$ kOe	-15.03	-7.71	-1.7	-3.75
MR (%)/ $T=5$ K, $H=40$ kOe	-17.87	-9.43	-2.91	-5.68

$M_s$  reduces from 18.07 e.m.u./g for  $x=0$  to 4.13 e.m.u./g for  $x=0.4$  (Table 1). The reduction in the value of  $M_s$  with indium composition in SFIMO compounds may be due to decrease in degree of Fe/Mo ordering or increase of anti-site defects in double perovskite structure. It is well known that the ASDs diminish  $M_s$  because the Fe spins in the Mo site anti-ferromagnetically couple with regular Fe spins. Ogale et al. [29] from Monte Carlo simulation study have reported that the anti-ferromagnetic Fe–O–Fe interaction grows with concentration of anti-site defects in  $\text{Sr}_2\text{FeMoO}_6$  leading to decrease in domain Fe contribution to the magnetization. Such a reduction in  $M_s$  was also reported when Ni, Cr, V, Ga, Mg and Al substituted at Fe site in  $\text{Sr}_2\text{FeMoO}_6$  [6,11,13,19,21,22]. The variation of  $M_r$  and  $H_c$  with indium composition is shown in the right side inset in Fig. 2. It can be noted that  $M_r$  decreases while  $H_c$  increases with increase of indium composition in SFIMO compounds. Similar increase of coercivity with composition was reported in Cr-doped  $\text{Sr}_2\text{FeMoO}_6$  compounds [30]. A comparison of variation of lattice parameters and magnetic properties is interesting. It is well known that the unit cell parameters are influenced by the size of dopant ion and independent of its magnetic properties. In the present investigation the variation in the lattice parameters is small and irregular which is attributed to cation/oxygen vacancies [26–28] or valence disproportion. However, when magnetic  $\text{Fe}^{2+}/\text{Fe}^{3+}$  is replaced by diamagnetic  $\text{In}^{3+}$ , the concentration of Fe–O–Fe and Fe–O–Mo patches decreases considerably leading to a decrease in the LFMR and other magnetic properties.

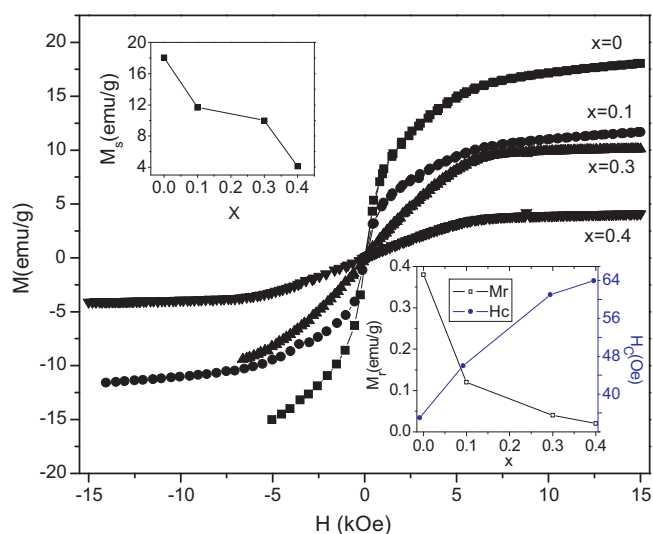


**Fig. 2.** Magnetic field dependence magnetization ( $M$ - $H$ ) curves for the  $\text{Sr}_2\text{Fe}_{1-x}\text{In}_x\text{MoO}_6$  ( $x=0, 0.1, 0.3$  and  $0.4$  wt.%) compounds obtained at room temperature. Left inset Fig shows the dependence of saturation magnetization ( $M_s$ ) while right inset figure shows remanent magnetization ( $M_r$ ) and coercivity ( $H_c$ ) with indium composition.

### 3.3. Resistivity and magnetoresistance studies

The resistivity ( $\rho$ ) data of  $\text{Sr}_2\text{Fe}_{1-x}\text{In}_x\text{MoO}_6$  ( $x=0, 0.1, 0.3$  and  $0.4$  wt.%) have been collected at different temperatures ranging from 5 to 300 K keeping magnetic field constant at 0, 10, 20 and 40 kOe. The variation of resistivity ( $\rho$ ) of  $\text{Sr}_2\text{Fe}_{1-x}\text{In}_x\text{MoO}_6$  with temperature at zero field is shown in Fig. 3 for all the samples. It can be seen from Fig. 3 that all these samples exhibit semiconductor behavior at 5 K and transform into metallic character as temperature is increased indicating a semiconductor-metallic transition. Similar results were obtained in the  $\text{Sr}_2\text{Fe}_{1-x}\text{Cr}_x\text{MoO}_6$  compounds [11]. It is noticed from Fig. 3 that the values of resistivity ( $\rho$ ) decreases considerable with increase of indium content in SFIMO materials except for the composition of indium  $x=0.4$ . The decrease in resistivity may be attributed to the increase in grain size that reduced the grain boundary on substitution of indium in SFMO [31]. However, the value of  $\rho$  at  $x=0.4$  is comparable with that of  $x=0$ . This may be attributed to impurities between the grain boundaries which may not have been detected in XRD.

The temperature dependence of MR (%) of  $\text{Sr}_2\text{Fe}_{1-x}\text{In}_x\text{MoO}_6$  ( $x=0, 0.1, 0.3$  and  $0.4$  wt.%) materials at a field of 10, 20 and 40 kOe are shown in Fig. 4(a), (b) and (c) respectively. MR (%) is defined as  $\text{MR}(\%) = \{[\rho(H, T) - \rho(0, T)] / \rho(0, T)\} \times 100$ . Here  $H$  denotes the applied field and  $\rho(0, T)$  and  $\rho(H, T)$  are the resistivity at zero field and  $H$  fields respectively at temperature  $T$ . The values of MR (%) at temperature 5 K and different fields at  $H=10, 20$  and  $40$  kOe are obtained from Fig. 4 and these values are included in Table 1 for all the compositions. The values of MR (%) at 5 K and at a low field  $H=10$  kOe (LFMR) are found to be -12.01, -6.18, -1.08, -2.78% for  $x=0, 0.1, 0.3$  and  $0.4$  respectively (Table 1). There-

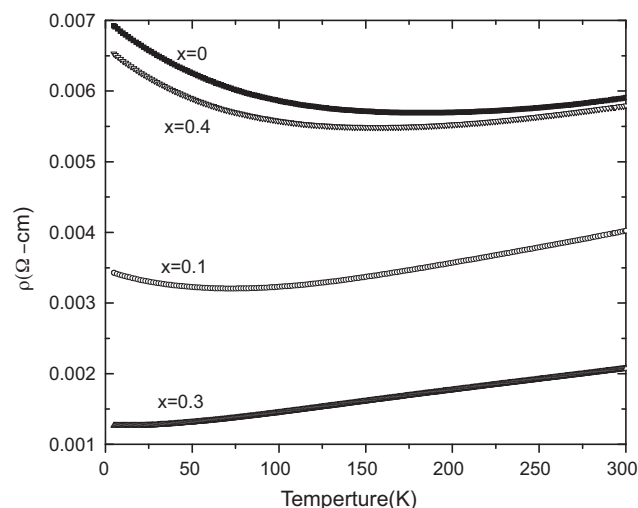


**Fig. 3.** Variation of resistivity of  $\text{Sr}_2\text{Fe}_{1-x}\text{In}_x\text{MoO}_6$  ( $x=0, 0.1, 0.3$  and  $0.4$  wt.%) samples at zero magnetic field with temperature.

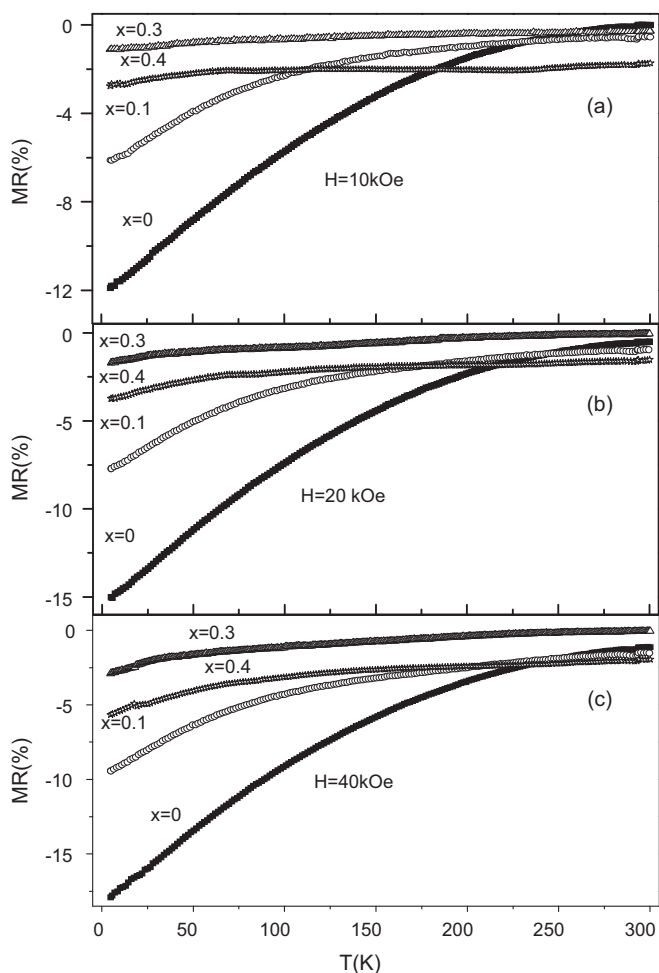


**Fig. 4.** Variation of MR (%) with temperature for  $\text{Sr}_2\text{Fe}_{1-x}\text{In}_x\text{MoO}_6$  ( $x=0, 0.1, 0.3$  and  $0.4$  wt.%) samples at an applied field of (a) 10 kOe, (b) 20 kOe and (c) 40 kOe.

fore in general, a decrease of MR (%) at low field with increase in indium concentration has been observed. Similar decrease of MR (%) with composition also was observed at 20 and 40 kOe as shown in Fig. 4(b) and (c) respectively in SFMO compounds. Similar trends have been reported for Ni, Cr and Mg doped SFMO materials [6,11,21]. These results could be understood in term of the model proposed by Garcia-Hernandez et al. [7]. They have related the observed linear dependence of LFMR on the saturation magnetization of  $\text{A}_{2-x}\text{A}'_x\text{FeMoO}_6$  systems to the anti-site disorder at the Fe and Mo sites and argued that the observation resulted from a spin-dependent crossing of intragranular barriers originated from the presence of anti-ferro magnetic (AF) Fe–O–Fe patches that naturally develop when anti-site disorder occurs in the double perovskites. As observed from magnetic measurements that magnetization decreases with indium composition ( $x$ ), which indicates the decrease in spin polarization of charge carriers leading to decrease of LFMR. This decrease in the spin polarization may be due to the suppression of Fe–O–Mo bonds upon indium doping, which may have impact on the half metallic character of these double perovskites. Therefore, the reduction in spin polarization may be the reason for the reduction in MR (%) as MR (%) is expected to increase with improvement in  $M_s$ . Therefore, in the present study, decrease of LFMR and  $M_s$  with indium composition may be due to reduction in spin polarization. It can be seen from Fig. 4 that increase in the magnitude of MR (%) with decrease of temperature suggests that the grain boundary effect dominates MR as temperature is decreased in SFMO.

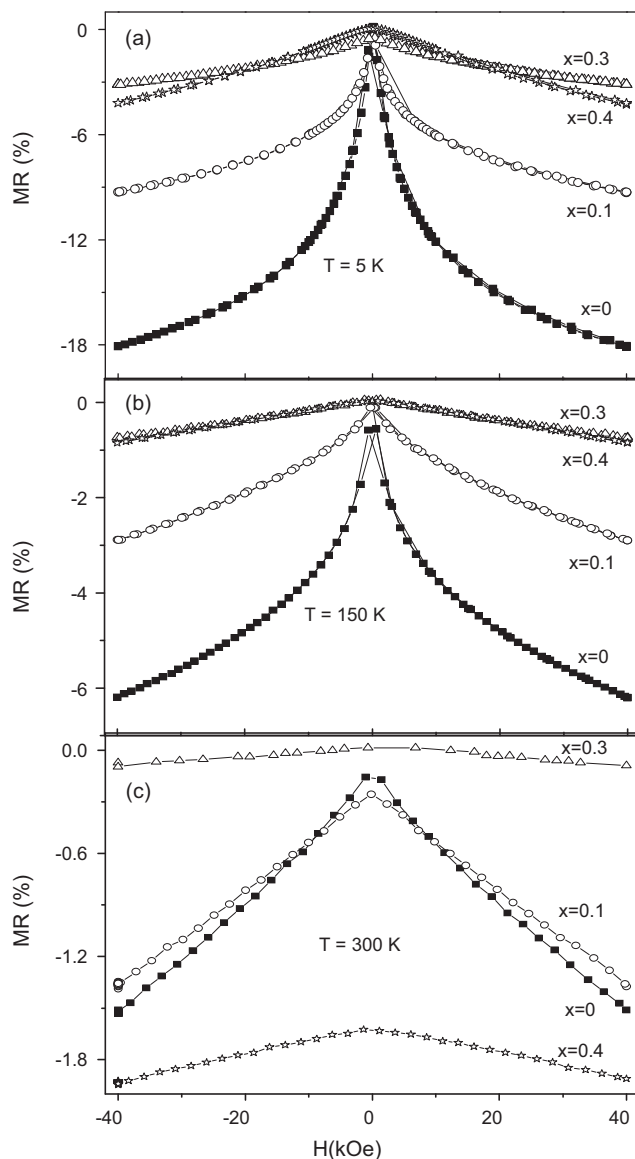


**Fig. 5.** Variation of MR (%) of  $\text{Sr}_2\text{Fe}_{1-x}\text{In}_x\text{MoO}_6$  ( $x=0, 0.1, 0.3$  and  $0.4$  wt.%) samples as a function of magnetic field at (a) 5 K, (b) 150 K and (c) 300 K.

The Magnetic field dependence of MR (%) for all the compounds in the magnetic field range of  $-40$  to  $40$  kOe at 5, 150 and 300 K and are shown in Fig. 5(a), (b) and (c) respectively. From Fig. 5(a), the value of MR (%) at a temperature of 5 K and at magnetic fields 10, 20 and 40 kOe have been determined and are included in Table 1. It is found that the MR (%) at 5 K increases with increase of magnetic field. The increase of MR (%) is due to the lowering of spin scattering at grain boundaries on application of magnetic field [7,21]. From Fig. 5(b) and (c), similar increase of MR (%) with magnetic field also can be seen at 150 and 300 K. From Table 1, it can be seen that the magnitude of MR (%) for composition  $x=0$  and  $x=0.4$  are  $-17.87$  and  $-5.68$  at a field of 40 kOe and temperature 5 K. This shows that the magnitude of MR (%) decreases with increase in indium composition in SFMO. Therefore, it may be concluded that magnitude of MR (%) increases with increase of magnetic field but the MR (%) decreases with increase of indium compositions. Similar trends have also been observed at 150 K and 300 K. The reduction in MR (%) by addition of indium can be attributed to increase of anti-site defects and reduction in spin polarization of charge carriers [6,7]. A good estimate of LFMR was difficult for  $x=0.4$  samples at

5 K (Table 1) due to nonlinearity of the MR (%) even at 40 kOe, hence it deviates from above trend.

#### 4. Conclusions

Indium doping in  $\text{Sr}_2\text{FeMoO}_6$  reduces the degree of ordering of Fe/Mo site and ASDs. The tetragonal distortion and the deviation of tolerance factor from unity are found to increase with indium composition in  $\text{Sr}_2\text{Fe}_{1-x}\text{In}_x\text{MoO}_6$  materials indicating addition of indium reduces the symmetry of the lattice. The  $M_s$  was found to decrease with the indium concentration in SFIMO materials. Reduction in LFMR with indium concentration has been observed in SFIMO materials. MR (%) was found to increase with increase of applied field while the same was found to increase with decrease in temperature. It may be concluded that the degree of ordering,  $M_s$  and MR (%) agreed well with each other.

#### Acknowledgements

The authors thank Dr. Rajeev Rawat and Dr. Alok Banerjee in UGC-DAE, Consortium for Scientific Research, Indore for providing magnetoresistance and magnetization facilities for present study and UGC-SERO, Hyderabad for providing financial assistance to carryout this work under the minor research project (File No. MRP-350/04 and Link No.1350). The authors also wish to thank the Head, Department of Physics, Osmania University and the Principal, Nizam College, Osmania University, Hyderabad for providing facilities. One of the authors (YM) is grateful to Dr. K. Ravindra, Principal, MallaReddy Institute of Technology and Science, Maisammaguda, Secunderabad for continual help and encouragement.

#### References

- [1] K.I. Kobayashi, T. Kimura, H. Sawada, K. Terakura, Y. Tokura, *Nature (Lond.)* 395 (1998) 677.
- [2] G.Y. Liu, G.H. Rao, X.M. Feng, H.F. Yang, Z.W. Ouyang, W.F. Liu, J.K. Liang, *J. Alloys Compd.* 353 (2003) 42–47.
- [3] D. Niebieskikwiat, D. Sanchez, A. Canerio, L. Morales, M. Vasquez- Mansilla, F. Rivadulla, L.E. Hueso, *Phys. Rev. B* 62 (2000) 3340.
- [4] Y. Tomioka, T. Okuda, Y. Okimoto, R. Kumai, K.I. Kobayashi, Y. Tokura, *Phys. Rev. B* 61 (2000) 422.
- [5] L. Balcells, J. Navarrp, M. Bibes, A. Roig, B. Martynez, J. Fontcuberta, *Appl. Phys. Lett.* 78 (2001) 781.
- [6] Anurag Gaur, G.D. Varma, H.K. Singh, *J. Alloys Compd.* 460 (2008) 581–584.
- [7] M. Garcya-Hernandez, J.L. Martynez, M.J. Martynez-Lope, M.T. Casais, J.A. Alons, *Phys. Rev. Lett.* 86 (2001) 2443.
- [8] R.C. Yu, P. Zhao, F.Y. Li, Z.X. Liu, J. Liu, C.Q. Jin, *Phys. Rev. B* 69 (2004) 214405.
- [9] K.I. Kobayashi, T. Okuda, Y. Tomioka, T. Kimura, Y. Tokura, *J. Magn. Mater.* 218 (2000) 17.
- [10] D. Rubi, C. Frontera, J. Nogues, J. Fontcuberta, *J. Phys. Condens. Mater.* 16 (2004) 3173.
- [11] X.M. Feng, G.H. Rao, G.Y. Liu, H.F. Yang, W.F. Liu, Z.W. Ouyang, J.K. Liang, *Phys. B* 344 (2004) 21–26.
- [12] J.H. Kim, G.Y. Ahn, Park.F S.I., C.S. Knn, *J. Magn. Mater.* 282 (2004) 295.
- [13] Q. Zhang, G.H. Rao, X.M. Feng, G.Y. Liu, Y.G. Xiao, Y. Zhang, J.K. Liang, *Solid State Commun.* 133 (2005) 223.
- [14] L. Chen, C.L. Yuan, J.M. Xue, J. Wang, *J. Phys. D: Appl. Phys.* 38 (2005) 4003.
- [15] C.L. Yuan, Y. Zhu, P.P. Ong, *J. Appl. Phys.* 91 (2002) 4421.
- [16] Y. Moritomo, H. Kusuya, A. Machida, E. Nishibori, M. Takata, M. Sakata, A. Nakamura, *J. Phys. Soc. Jpn.* 70 (2001) 3182.
- [17] Y. Sui, X.J. Wang, Z.N. Qian, J.G. Cheng, Z.G. Liu, J.P. Miao, Y. Li, W.H. Su, C.K. Ong, *Appl. Phys. Lett.* 85 (2004) 269.
- [18] A. Pena, J. Gutierrez-Martinez, J.M. Barandian, T. Hernandez, T. Rojo, *J. Phys. Condens. Mater.* 13 (2001) 6535.
- [19] M.F. Lu, J.P. Wang, J.F. Liu, S. Wei, X.F. Hao, D.F. Zhou, X.J. Liu, Z.J. Wu, M. Jian, *J. Alloys Compd.* 428 (2007) 214–219.
- [20] H. Chang, M. Garcia-Hernandez, M. Retuerto, J.A. Alonso, *Phys. Rev. B* 73 (2006) 104417.
- [21] F. Sher, A. Venimadhav, M.G. Blamire, B. Dabrowski, S. Kolesnik, J. Paul Attfield, *Solid State Sci.* 7 (2005) 912–919.
- [22] E.K. Hemery, G.V.M. Williams, H.J. Trodal, *Phys. B* 394 (2007) 74–80.
- [23] J. Mahai, C. Vazquez, J. Mirza, A. Lopez-Quentela, J. Rivas, T.E. Jones, S.B. Oseroff, *J. Appl. Phys.* 75 (1994) 6757.
- [24] W.H. Song, J.M. Dai, S.L. Ye, K.Y. Wang, J.J. Du, Y.P. Sun, *J. Appl. Phys.* 89 (2001) 7678.
- [25] C.L. Yuan, Y. Zhu, P.P. Ong, *Appl. Phys. Lett.* 82 (2003) 934.
- [26] J. Topfer, J.B. Goodenough, *Chem. Mater.* 9 (1997) 1467.
- [27] J.A.M. van Roosmalen, P. van Vlaanderen, E.H.P. Cordfunke, W.L. Ijdo, D.J.W. Ijdo, *J. Solid State Chem.* 114 (1995) 516.
- [28] Y. Takeda, K. Kanno, T. Takada, O. Yamamoto, M. Takano, N. Nakayama, Y. Bando, *J. Solid State Chem.* 63 (1986) 237.
- [29] A.S. Ogale, S.B. Ogale, R. Ramesh, T. Venkatesan, *Appl. Phys. Lett.* 75 (1999) 537.
- [30] Je Hoon Kim, Geun Young Ahn, Seung-Iel Park, Chul Sung Kim, *J. Magn. Mater.* 282 (2004) 295–298.
- [31] N. Aanantharamaih, Ph.D. Thesis (2005) Dept of Physics, Osmania University, Hyderabad, India.